JLB

Brief Conclusive Report

Dynamics of dendritic cell-derived vesicles: high-resolution flow cytometric analysis of extracellular vesicle quantity and quality

Esther N. M. Nolte-'t Hoen, Els J. van der Vlist,* Mieke de Boer-Brouwer,* Ger J. A. Arkesteijn,† Willem Stoorvogel,* and Marca H. M. Wauben*,[1]*

Departments of *Biochemistry & Cell Biology and †Immunology, Faculty of Veterinary Medicine, Utrecht University, Utrecht, The Netherlands

RECEIVED SEPTEMBER 29, 2011; REVISED OCTOBER 31, 2012; ACCEPTED DECEMBER 1, 2012. DOI: 10.1189/jlb.0911480

ABSTRACT

Nano-sized membrane vesicles are secreted by many cell types. These vesicles can serve as carriers of cellular information. DC-derived vesicles can be targeted to other immune cells and modify their function. Accurate analysis of quantitative and qualitative changes in EV production by DC upon different activation stimuli is needed to further reveal the immune regulatory properties of DC-derived EVs. However, methods for reliable quantification of individual EVs and for analysis of the heterogeneity of EV populations are limited. With our recently developed high-resolution flow cytometry-based method, we can perform a high-throughput, multiparameter, and quantitative analysis of individual EVs. With the use of this novel technique, we show that despite previous assumptions, stimulation with bacterial LPS increases EV release by DC. Furthermore, we demonstrate heterogeneity in DC-derived EVs regarding their buoyant density and MHC class II content. Finally, we show that cognate interaction between LPS-stimulated DC and CD4$^+$ T cells affects both the quantity and quality of LPS DC-derived EVs present in the culture supernatant. These data indicate that flow cytometry-based analysis of individual EVs is a valuable, novel tool to study the dynamics of EV secretion and composition, offering great opportunities to unveil the function of immune cell-derived EVs. *J. Leukoc. Biol.* 93: 395–402; 2013.

Introduction

Eukaryotic cells can release different vesicle subsets (50–1000 nm), which are either shed from the plasma membrane or exocytosed by fusion of late endosomal compartments (multivesicular bodies) with the plasma membrane (exosomes) [1]. These EVs can be detected in cell culture conditioned medium and in a large range of body fluids [1]. EVs are secreted by a wide variety of cells, including APCs, such as B cells and DCs (reviewed in refs. [1, 2]). Evidence is accumulating that the pool of vesicles released by cells into the extracellular milieu is heterogeneous. Cells may regulate the composition of this vesicle pool by releasing vesicles from the endosomal compartment or the plasma membrane. Alternatively, cells may produce phenotypically different EV subpopulations within one subcellular compartment. The resulting heterogeneity in EV populations may explain why different vesicle-associated proteins distribute unequally within the classical range of densities described for exosomes [3, 4].

The function of EVs mainly depends on the EV cargo (proteins, lipids, and RNA), which is determined by the nature and activation status of the producing cell (reviewed in refs. [1, 2]). Various studies describe differences in the molecular make-up and function of EVs secreted by differentially activated DCs. EVs derived from immature DCs have been used as cell-free vaccines that can elicit T cell responses and inhibit tumor growth in mice [5, 6]. However, such immature DC-derived EVs cannot directly stimulate T cell responses but need to be transferred to DCs [7, 8]. Upon stimulation with bacterial LPS, DCs secrete EVs that are more potent inducers of T cell responses than immature DC EVs [9, 10]. Based on these findings, a second generation of activated DC-derived EVs with enhanced immune stimulatory properties is now being developed for clinical application [11].

Besides functional analysis of APC-derived EVs, the identification of triggers for EV secretion is crucial to understand the physiological role of these EVs in immune regulation. Based on total protein content analysis, Western blotting, ELISA, or bead-capture flow cytometric analysis for quantification of EVs, it has been postulated that microbial stimulation of DCs decreases EV secretion. This is different from B cells, which increase EV secretion upon microbial stimulation [10, 12–15]. In

Abbreviations: EV=extracellular vesicle, FL=fluorescence, FSC=forward scatter, MHCII-hi/-int/-lo=high/intermediate/low amount of Major Histocompatibility Complex class II, PSI=pounds/square inch, R1=NIH 3T3 cells

The online version of this paper, found at www.jleukbio.org, includes supplemental information.

1. Correspondence: Utrecht University, Faculty of Veterinary Medicine, Dept. of Biochemistry & Cell Biology, Yalelaan 2, 3584CM Utrecht, The Netherlands. E-mail: m.h.m.wauben@uu.nl

contrast to the reported differences in EV secretion between B cells and DCs after microbial stimulation, it has been proposed that both APC types increase EV secretion upon cognate interaction with $CD4^+$ T cells [13, 16]. However, a major obstacle in studying the dynamics of EV release and their molecular contents is the lack of reliable methods to quantify the number of secreted EVs and the number of molecules/vesicle.

The currently used quantification methods are based on bulk analysis of EVs rather than on quantification of individual EVs. Bulk analysis of EVs is, however, hampered by the lack of invariable vesicle-associated "household" markers. Consequently, bulk analysis-based quantification strategies cannot discriminate between changes in EV numbers and changes in the number of molecules/EV.

We recently developed a flow cytometry-based method for multiparameter analysis of individual EVs. With this method, quantification of vesicles, independently of their protein content, can be combined with the detection of specific proteins on individual vesicle subpopulations [17, 18]. This technique therefore offers unique opportunities for the identification of different EV subpopulations.

In the present study, we used this novel method to analyze the dynamics of secretion and composition of DC-derived EVs upon stimulation of DCs with LPS and during interaction with cognate $CD4^+$ T cells.

MATERIALS AND METHODS

Cell culture

Bone marrow-derived DCs were generated from C57BL/6 mice, as described [19], with minor modifications. In short, bone marrow cells were maintained in IMDM, supplemented with 2 mM UltraGlutamine (BioWhittaker, Lonza, Switzerland), 10% heat-inactivated FCS (Sigma-Aldrich, St. Louis, MO, USA), 100 IU/ml penicillin and 100 mg/ml streptomycin (Gibco, Life Technologies, Grand Island, NY, USA), 50 μM β-ME, and 30% conditioned medium from GM-CSF producing R1. At Days 2, 6, and 8, medium was added or replaced. On Day 9, nonadherent cells were collected by gentle pipetting and plated in new dishes with fresh medium. When indicated, cells were activated with 10 μg/ml LPS on Day 13. Semiadherent and nonadherent cells were harvested on Day 14 and replated for EV production in EV-depleted medium containing overnight, ultracentrifuged (100,000 *g*) FCS and GM-CSF containing conditioned R1 medium (to deplete bovine and R1 cell EV). The p53-specific $CD4^+$ T cell clone, generated in a C57BL/6 $p53^{-/-}$ mouse [20] and provided by Prof. Cornelis. Melief (Leiden University Medical Center, Leiden, The Netherlands), was cultured as described previously [16]. For (non-)cognate LPS DC/T cell coculture conditions, DCs were incubated with (cognate) or without (noncognate) 2.5 μM p53 peptide (aa 77–96) in the presence of 10 μg/ml LPS on Day 13 and harvested and mixed in a 1:1 ratio with T cells on Day 14 and cocultured for 20 h. Where indicated, T cells were labeled with 0.5 μM CFSE (Invitrogen, Carlsbad, CA, USA) for 15 min at 37°C. All cultures were maintained at 37°C, 5% CO_2. Experiments were approved by the Institutional Ethical Animal Committee at Utrecht University (Utrecht, The Netherlands).

EV isolation and labeling

EVs were collected from the culture supernatants of 3×10^6 DC or 3×10^6 DC, cocultured with 3×10^6 T cells by differential centrifugation [21]. In short, cells were removed by two sequential centrifugations at 200 *g* for 10 min. Collected supernatant was subsequently centrifuged two times at 500 *g* for 10 min, followed by 10,000 *g* for 30 min. EVs were finally pelleted by ultracentrifugation at 100,000 *g* for 65 min in a SW40 rotor (Beckman Coulter, Brea, CA, USA) and resuspended in 20 μl PBS containing 0.2% BSA from a stock solution that had been cleared from aggregates by ultracentrifugation. EVs were fluorescently labeled with 7.5 μM PKH67 (Sigma-Aldrich) in an end volume of 200 μl, following the manufacturer's recommendations. In case of antibody staining, EVs resuspended in 20 μl PBS/0.2% BSA were incubated with 0.5 μg PE-labeled anti-mouse MHC class II antibody (clone M5/114; eBioscience, San Diego, CA, USA) for 45 min at room temperature, after which, PKH67 labeling was performed as described above. EVs were then mixed with 2.5 M sucrose, overlaid with a linear sucrose gradient (2.0–0.4 M sucrose in PBS), and floated into the gradient by centrifugation in a SW40 tube (Beckman Coulter) for 16 h at 192,000 *g*. Gradient fractions of 1 ml were collected from the bottom of the tube, diluted 20-fold with PBS, and analyzed by flow cytometric analysis. Fraction densities were determined by refractometry.

Flow cytometric analysis of EV

The BD Influx flow cytometer (Becton Dickinson, Brussels, Belgium) was used for flow cytometric analysis of individual EVs [17]. Light scattering was measured in a straight line with the laser excitation beam with a collection angle of 15–25° (wide-angle FSC). Samples were run at low pressure (5 PSI on the sheath fluid and 4.2 PSI on the sample) using a 140-μm nozzle. For all measurements, the system was triggered on the fluorescence signal derived from the fluorescently labeled EVs, and thresholding was applied on this fluorescence channel. Fluorescence thresholding was based on measuring 0.22 μm-filtered PBS, allowing an event rate of not more than six events/s. For calibration of the machine, we established fixed positions for fluorescent 100- and 200-nm polystyrene beads (yellow-green fluorescent FluoSpheres; Invitrogen) in wide-angle FSC/side-scatter and wide-angle FSC/FL1 plots as a reference. For all analyses, light-scattering detection was performed in log mode. Samples were measured at event rates lower than 10,000 events/s. Sucrose gradient fractions were diluted in PBS and vortexed before measurement. The two bottom fractions of the gradient were left out, as unbound staining reagents in these fractions severely hampered detection of labeled membrane vesicles. Sample measurements were performed as described before [18]. PE-labeled antibodies were measured by excitation with the 561-nm laser and using a 585/42 band-pass filter.

Western blot analysis

Sucrose gradient fractions were diluted with PBS and centrifuged for 65 min at 100,000 g using a SW60 rotor (Beckman Coulter). The pellets were solubilized in nonreducing SDS-PAGE sample buffer and separated by 12.5% SDS-PAGE. Proteins were transferred to PVDF membranes (Millipore, Billerica, MA, USA), which were blocked in PBS containing 5% (w/v) nonfat dry milk (Protifar plus; Nutricia, Amsterdam, The Netherlands) and 0.1% (v/v) Tween-20, and MHCII was detected by immunoblotting. Rabbit polyclonal antibody directed against the cytoplasmic domain of mouse MHCII-β was kindly provided by Dr. Nicolas Barois [22] and detected using HRP-conjugated secondary antibody (Pierce Biotechnology, Thermo Fisher Scientific, Rockford, IL, USA). CD86 was detected by immunoblotting with biotinylated anti-CD86 (GL1; eBioscience) and HRP-conjugated streptavidin. Proteins were detected using SuperSignal West Pico Chemiluminescent Substrate (Pierce Biotechnology, Thermo Fisher Scientific). Protein levels were quantified by densitometry using Quantity One Basic software (Bio-Rad, Hercules, CA, USA).

Flow cytometric analysis of cells

Cells were harvested and incubated with antibodies as indicated for 30 min on ice in PBS containing 1% BSA (PBS–BSA). PE-conjugated anti-I-Ab (clone M5/114), anti-TCR (CTVB11), or anti-CD69 (H1.2F3) and the corresponding isotype control antibodies were from eBioscience. Cells were analyzed using FACSCalibur and CellQuest (Becton Dickinson) and FCS Express software (De Novo Software, Los Angeles, CA, USA).

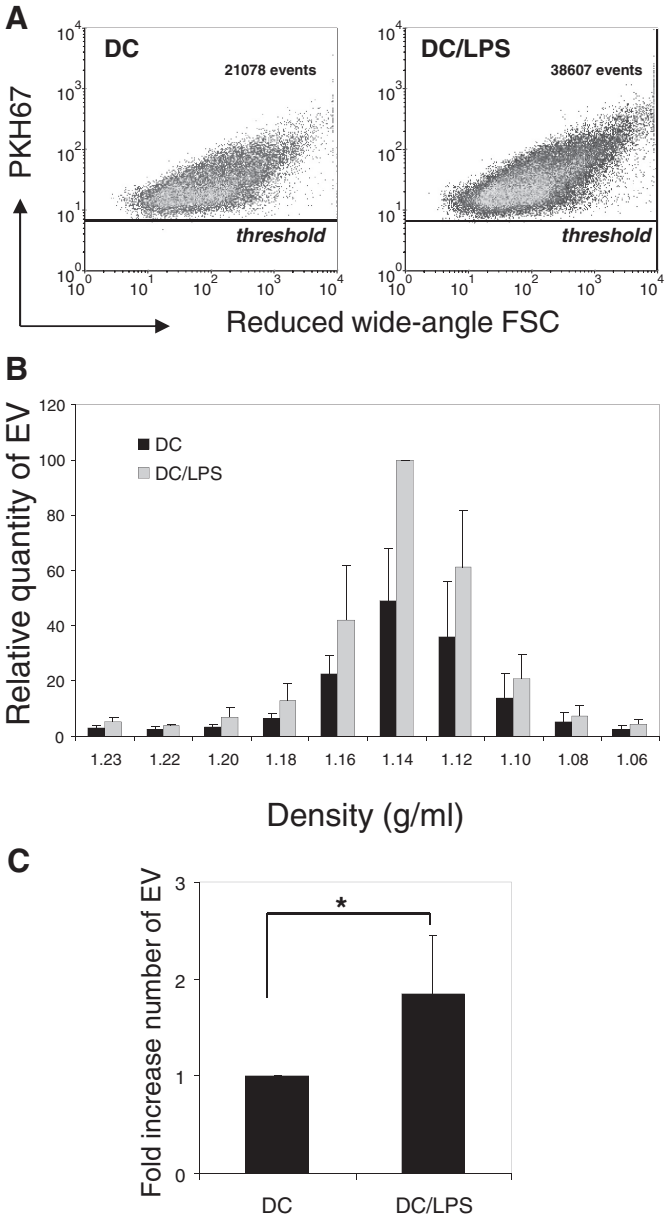

Figure 1. DCs increase EV secretion in response to LPS stimulation. EVs were isolated from culture supernatants of nonstimulated DCs or LPS- stimulated DCs (DC/LPS), fluorescently labeled with PKH67, and floated into a sucrose gradient. Sucrose gradient fractions were analyzed by high-resolution flow cytometric analysis using a threshold on PKH67 fluorescence. (A) Dot plots of reduced wide-angle FSC versus PKH67 fluorescence representing fluorescent EVs released by nonactivated DCs (left) or LPS-activated DCs (right) from pooled fractions with densities of 1.11–1.18 g/ml. Indicated are the number of events measured in 30 s. (B) Time-based quantification of fluorescent EVs detected in different gradient fractions. Numbers of detected events were normalized to the number of EVs released by LPS-activated DCs with a buoyant density of 1.14 g/ml (set to 100%). Indicated are the relative quantities of EVs (average±SD) measured in 30 s. Data are from four independent experiments. (C) Average and SD of the number of EVs detected in supernatants of nonstimulated versus LPS-stimulated DCs of $n = 6$ independent experiments. Indicated is the factor increase in number of EVs (pools of 1.11–1.18 g/ml sucrose fractions) secreted by LPS-stimulated DCs relative to nonstimulated DCs (nonstimulated DC EVs were set to 1). $^*P < 0.05$.

Statistics

The numbers of EVs (pooled fractions 1.11–1.18 g/ml; $n=6$ independent experiments), as well as differences in MHCII geomean intensity (per fraction; $n=6$) and percentage of MHCII-positive vesicles (per fraction; $n=6$) produced by DCs upon different activation stimuli, were compared statistically using a two-tailed, paired Student's *t*-test. Differences in MHCII geomean intensity between fractions within one activation condition ($n=6$) were compared using a one-way ANOVA with Tukey's post hoc tests. Differences in the number of MHCII-positive vesicles secreted by LPS-activated DCs, cultured alone or in the presence of $CD4^+$ T cells (total numbers or numbers in arbitrary gates), were tested with a one-sample *t*-test. All tests were two-tailed, and *P* values <0.05 were considered statistically significant. Asterisks indicate *P* values: $^*P < 0.05$; $^{**}P < 0.01$; or $^{***}P < 0.001$.

RESULTS AND DISCUSSION

We first determined how LPS stimulation of DCs affected the number of secreted EVs. EVs secreted by murine bone marrow-derived DCs were isolated from a cell culture supernatant by differential centrifugation and subsequently labeled for high-resolution flow cytometric analysis of individual EVs [17]. As the light scattering of nano-sized membrane vesicles overlaps with noise signals, EVs were labeled with the general lipid dye PKH67 and floated by centrifugation into an overlaid sucrose gradient [16, 17]. Based on PKH67 fluorescence, labeled DC EVs could be detected above the fluorescence threshold (**Fig. 1A**). Quantification by time-based flow cytometric analysis demonstrated that the vast majority of vesicles produced by nonstimulated and LPS-stimulated DCs equilibrated at densities of 1.11–1.18 g/ml (Fig. 1B), corresponding to the representative density range of EVs [1]. Importantly, we found that LPS stimulation of DCs led to a 1.9-fold increase in the number of EVs in the culture supernatant as compared with EVs secreted by nonstimulated DCs (Fig. 1B and C). From a physiological point of view, our finding that LPS stimulation of DCs increases EV production is important, as such activated DC-derived EVs with strong T cell-stimulatory capacity could actively contribute to amplification of immune responses. Our results seem to contradict previous reports, suggesting a reduction in DC EV secretion upon LPS stimulation [10, 12, 14]. Differences in EV isolation procedures, such as the addition of filtration steps or low-temperature storage of cell culture supernatant [10, 14], could explain the disparity in results. More importantly, previous studies used total protein assays and Western blotting to assess the amount of EVs. Such assays are, however, far from ideal for quantification of EVs. First, phospholipids present in EVs and detergents commonly used to disrupt vesicle membranes can cause considerable errors in the measured protein values [23]. Second, specific protein-based quantification of EVs by Western blotting is difficult, as the amount of a specific protein may vary between different EV subsets. Importantly, our flow cytometry-based data were recently corroborated by Soo et al. [24], who demonstrated with a different EV quantification technique (nanoparticle tracking analysis) and using DCs from a different source (human monocyte-derived DCs) that the number of released vesicles increased upon DC stimulation with LPS.

Next, we investigated whether LPS-stimulated and nonstimulated DCs release vesicles that differ in their MHCII content by combining flow cytometric analysis of EV numbers and MHCII protein detection by Western blotting (**Fig. 2A** and **B**). The observed increase in the number of EVs released by LPS-stimulated DCs was accompanied by an overall increase in MHCII signal obtained by Western blotting. However, within the population of EVs released by nonstimulated DCs, we noticed that

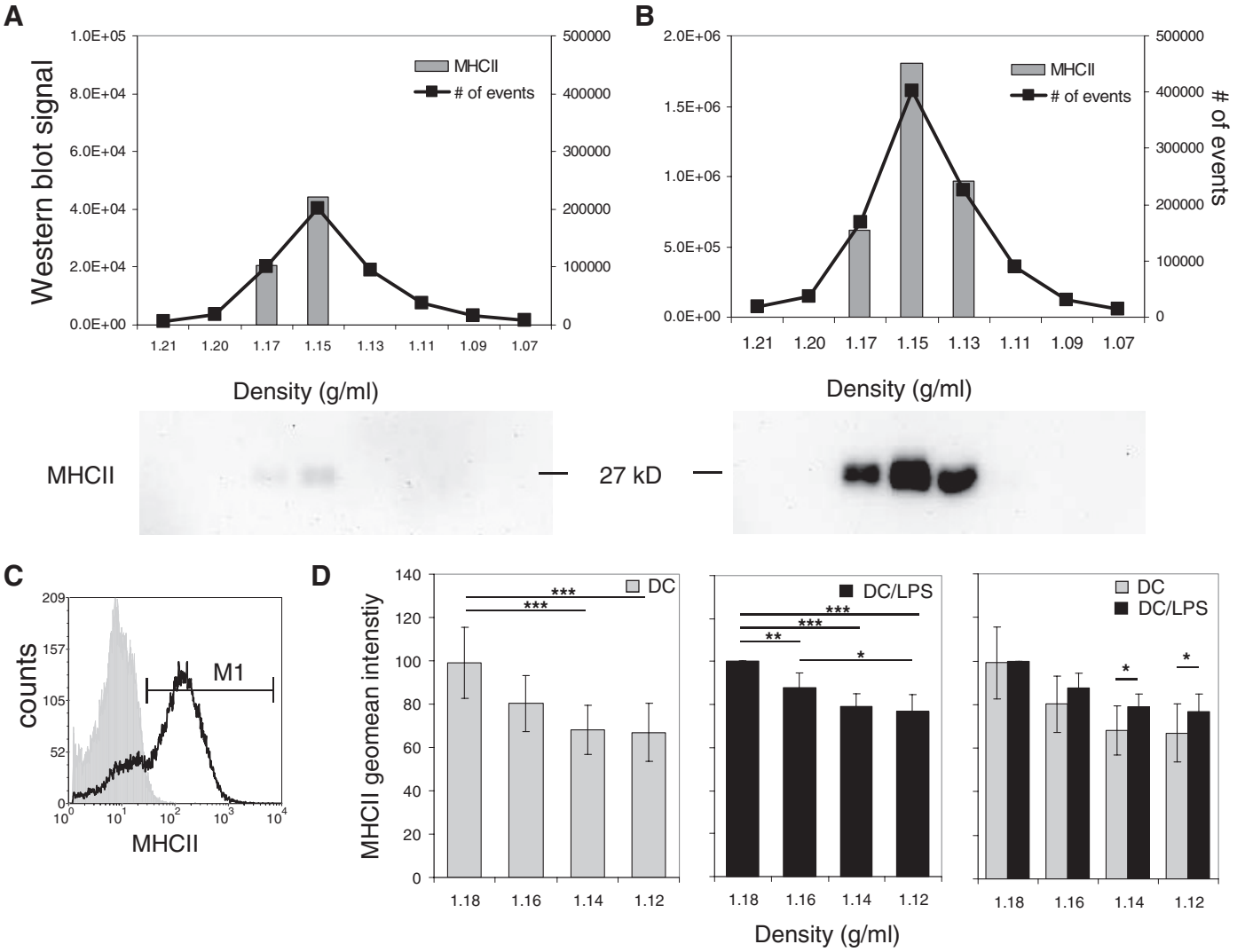

Figure 2. Heterogeneity within DC EV populations and between EV populations secreted by differently activated DCs. EVs were isolated from culture supernatants of nonstimulated DCs or LPS-stimulated DCs, fluorescently labeled with PKH67 (A and B) or PKH67 and PE-conjugated anti-MHCII (C–E), and floated into a sucrose gradient. Sucrose gradient fractions were analyzed on a high-resolution flow cytometer using a threshold on PKH67 fluorescence. (A and B) Flow cytometric and Western blot analysis of sucrose gradient fractions containing EV derived from nonstimulated DCs (A) or LPS-stimulated DCs (B). The left *y*-axis (in A) indicates the MHCII protein levels as quantified by Western blotting (bars and pictures below the graphs). The right *y*-axis (in B) indicates the number of events detected in 30 s by the flow cytometric approach (line). (C) Histogram representing anti-MHCII (black line)- or isotype control antibody (gray solid)-labeled EVs derived from LPS-activated DCs, pooled from 1.11 g/ml to 1.18 g/ml density fractions. MHCII-positive EVs were gated (gate M1) based on the isotype control staining. (D) EVs derived from nonstimulated and LPS-stimulated DCs were compared for MHCII labeling intensity. Indicated are the geometric mean fluorescence intensities (average±SD) of MHCII staining in each of the indicated gradient fractions. Data were normalized to the intensity of the EVs with a buoyant density 1.18 g/ml (n=6 independent experiments). MHCII-positive events were gated as in C. (E) The percentage of MHCII-positive EVs was determined as shown in C. Indicated is the comparison of the percentages of MHCII-positive EVs (average±SD of six independent experiments) released by nonstimulated and LPS-stimulated DCs. *$P < 0.05$; **$P < 0.01$; ***$P < 0.001$.

density fractions containing similar numbers of EVs (densities 1.13 and 1.17 g/ml) displayed substantial differences in MHCII protein levels (Fig. 2A). This could be a result of differences in the MHCII content of EVs residing in these different density fractions. Therefore, the MHCII content of antibody-stained individual EVs was determined using flow cytometry-based analysis (Fig. 2C). The geometric mean MHCII intensity of MHCII-positive EVs varied between the different fractions, with EVs floating at the highest density (1.18 g/ml) containing the highest amount of MHCII (Fig. 2D). Furthermore, the MHCII content of the lower density EVs from LPS-activated DCs was higher compared with those EVs derived from nonstimulated DCs (Fig. 2D). In addition, the percentage of MHCII-positive EVs released by LPS-activated DCs was substantially higher compared with nonactivated DCs (Fig. 2E). Like MHCII, also the amount of CD86 released in the culture supernatant increased upon DC activation, as measured by Western blotting (Supplemental Fig. 1). However, both the absence of high-affinity flow cytometry antibodies for costimulatory molecules and perhaps the lower abundance of these molecules on the vesicles currently prohibit their detection on individual EVs using our flow cytometry-based assay. The present data indicate that heterogeneity exists not only between EVs produced by DCs undergoing different modes of stimulation but also between EVs produced during one culture condition. Collectively, our data indicate that different EV subsets produced by one cell type can be identified based on buoyant density combined with high-resolution flow cytometric analysis of the specific protein content of individual EVs.

We previously showed that during cognate interactions of DCs with $CD4^+$ T cells, EV-associated MHCII is released into the culture supernatant [16, 25]. Besides this, part of the released MHCII is recruited to other DCs [7, 9, 16, 25, 26] and part to interacting T cells in a LFA-1-dependent fashion [25]. By using flow cytometry-based analysis of individual EVs, we here investigated whether cognate interactions between LPS-activated, antigen-loaded DCs and antigen-experienced $CD4^+$ T cells resulted in selective recruitment of specific subsets of DC EVs to these T cells. First, we compared the quantity and quality of MHCII-carrying EVs recovered from the DC culture supernatant in the absence or presence of cognately interacting T cells. By antibody staining for MHCII, MHCII-positive DC-derived EVs could be distinguished from MHCII-negative, T cell-derived EVs [17]. With the use of this method, we found a strong decrease in the number of MHCII-positive EVs in the extracellular milieu when LPS-activated DCs were cultured in the presence of cognately interacting T cells (**Fig. 3A** and **B**). Importantly, this effect was strictly dependent on cognate antigen recognition (Fig. 3B). Flow cytometric analysis of CFSE-labeled $CD4^+$ T cells cocultured with nonlabeled, antigen-pulsed, LPS-stimulated DCs revealed that the T cells were activated (indicated by reduced TCR expression and increased CD69 expression) and that substantial amounts of DC-derived MHCII were recruited to the T cell surface (**Fig. 4A**). We next investigated whether the cognate T cells selectively recruited specific EV subpopulations released by the interacting DCs. Hence, we investigated the phenotype of DC EVs present in the supernatant of DCs or DC–T cell cultures. To quantify EVs

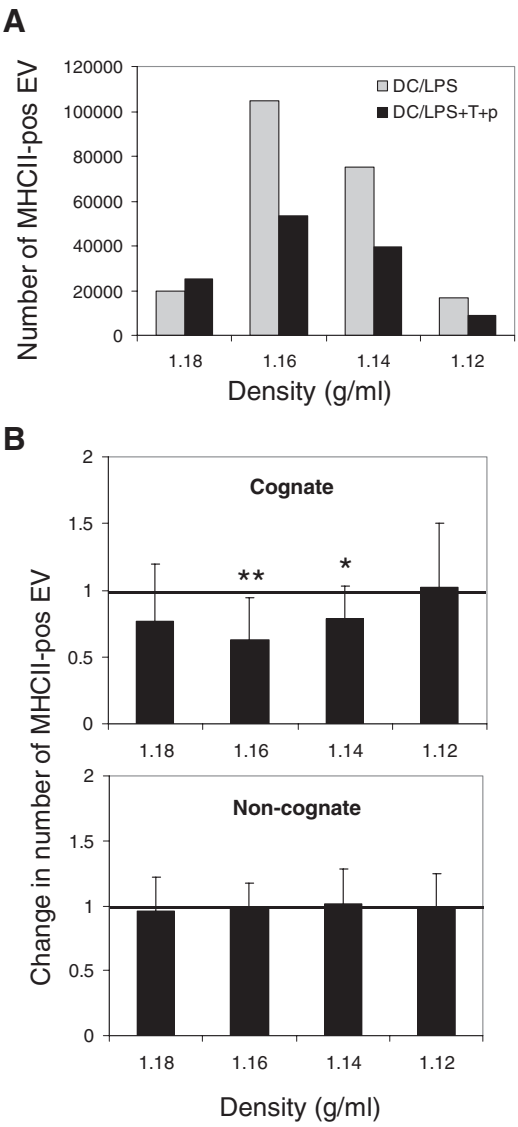

Figure 3. Quantitative and qualitative analysis of DC EVs secreted during cognate interactions with T cells. EVs were isolated from culture supernatants of LPS-stimulated DCs, cultured alone or pulsed with specific peptide and cocultured with cognate antigen-experienced $CD4^+$ T cells (T+p). EVs were fluorescently labeled with PKH67 and PE-labeled anti-MHCII and floated to equilibrium into a sucrose gradient. Sucrose gradient fractions were analyzed by high-resolution flow cytometric analysis using a threshold on PKH67 fluorescence. (A) Time-based quantification of MHCII-positive (pos) events detected in different gradient fractions of (cocultured) LPS-stimulated DCs. Indicated are the numbers of events measured in 30 s. One representative experiment out of nine is shown. (B) Ratios of the number of MHCII-positive EVs in culture supernatants of cognate DC–T cell cultures (upper) or noncognate cultures (lower) over the number of MHCII-positive EVs in supernatants of cultures of LPS-stimulated DCs alone. Indicated are average values ± SD of nine (cognate interactions) or four (noncognate interactions) independent experiments. $*P < 0.05$; $**P < 0.01$.

carrying different levels of MHCII, arbitrary gates were set for EVs containing low, intermediate, or high levels of MHCII in the different density fractions (Fig. 4B). In cocultures of LPS-activated DCs with cognate T cells, EVs with buoyant densities

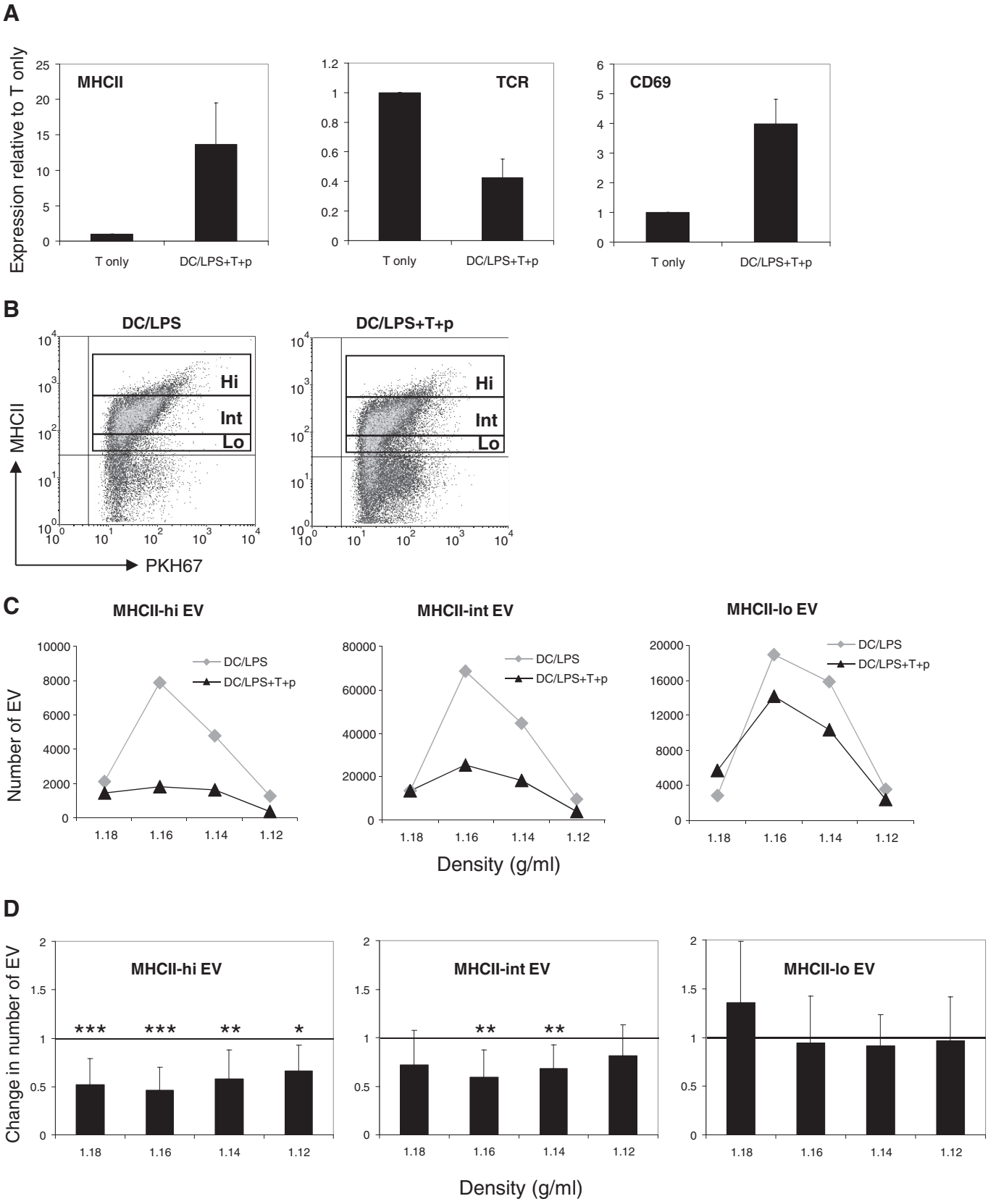
A
Expression relative to T only
MHCII
TCR
CD69
T only
DC/LPS+T+p
B
DC/LPS
DC/LPS+T+p
Hi
Int
Lo
MHCII
PKH67
C
MHCII-hi EV
MHCII-int EV
MHCII-lo EV
Number of EV
DC/LPS
DC/LPS+T+p
Density (g/ml)
D
Change in number of EV
MHCII-hi EV
MHCII-int EV
MHCII-lo EV
Density (g/ml)

of 1.12–1.18 g/ml, which contained the the highest amount of MHCII (MHCII-hi), were eliminated most efficiently from the culture supernatant (Fig. 4C and D). A smaller decrease was observed for the number of 1.14–1.16 g/ml EVs with intermediate MHCII levels, whereas the numbers of MHCII-lo EVs in the coculture supernatant remained unchanged. These data suggest that MHCII-hi EVs had been recruited preferentially onto the T cells. Alternatively, interactions with T cells could have induced the DCs to produce relatively more EVs with lower MHCII contents. This seems less likely, as the numbers of MHCII-lo EVs recovered from supernatants of LPS-activated DCs in the presence or absence of T cells were not affected significantly. Based on these data, we conclude that $CD4^+$ T cells selectively capture DC-derived EVs containing the higher amounts of MHCII during cognate interactions with LPS–DC. It is currently not known whether T cells received triggers from the LPS–DC to increase the expression of receptors involved in EV binding, e.g., LFA-1 [25], or whether MHCII-hi EVs contain higher levels of cognate MHCII–peptide complexes or other proteins involved in T cell binding. Generally, DC EVs, which are not directly recruited to neighboring or interacting DCs and T cells, are available for targeting to other cells. We are currently investigating whether DC EVs, secreted in the extracellular environment during cognate interactions between LPS-stimulated DCs and $CD4^+$ T cells, have different immune regulatory properties.

Conclusively, we show here that with a high resolution, multiparameter flow cytometry-based method to analyze individual EVs, detailed information can be obtained regarding the number and heterogeneity of EVs secreted by DCs undergoing different modes of activation. In contrast to previously used techniques, this method allows the uncoupling of quantitative and qualitative measurements in studying secreted EVs. This is particularly important when the protein composition of EVs changes as a result of environmental triggers, such as during DC activation. With the use of this flow cytometric approach, we showed that DCs increase EV secretion upon LPS stimulation. In addition, we obtained evidence that the EV population derived from cells in one culture condition contains subsets that differ in buoyant density and protein content. The discriminative ability of our technique further allowed us to demonstrate that during cognate DC–T cell interactions, T cells preferentially capture subpopulations of DC-derived EVs with higher levels of MHCII. Based on these findings, we are confident that high-resolution flow cytometry-based analysis of individual EVs will open up new avenues to further unravel the role of EVs in immune regulation.

AUTHORSHIP

E.N.M.N.H., W.S., and M.H.M.W. designed the study. E.N.M.N.H., E.J.V., M.B-B., and G.J.A.A. performed experiments. E.N.M.N.H., E.J.V., and M.H.M.W. wrote the paper.

REFERENCES

1. Thery, C., Ostrowski, M., Segura, E. (2009) Membrane vesicles as conveyors of immune responses. *Nat. Rev. Immunol.* **9,** 581–593.
2. Nolte-'t Hoen, E. N., Wauben, M. H. (2012) Immune cell-derived vesicles: modulators and mediators of inflammation. *Curr. Pharm. Des.* **18,** 2357–2368.
3. Escola, J. M., Kleijmeer, M. J., Stoorvogel, W., Griffith, J. M., Yoshie, O., Geuze, H. J. (1998) Selective enrichment of tetraspan proteins on the internal vesicles of multivesicular endosomes and on exosomes secreted by human B-lymphocytes. *J. Biol. Chem.* **273,** 20121–20127.
4. Bobrie, A., Colombo, M., Krumeich, S., Raposo, G., Théry, C. (2012) Diverse subpopulations of vesicles secreted by different intracellular mechanisms are present in exosome preparations obtained by differential ultracentrifugation. *J. Extracell. Vesicles* **1,** 18397.
5. Zitvogel, L., Regnault, A., Lozier, A., Wolfers, J., Flament, C., Tenza, D., Ricciardi-Castagnoli, P., Raposo, G., Amigorena, S. (1998) Eradication of established murine tumors using a novel cell-free vaccine: dendritic cell-derived exosomes. *Nat. Med.* **4,** 594–600.
6. Chaput, N., Schartz, N. E., Andre, F., Taieb, J., Novault, S., Bonnaventure, P., Aubert, N., Bernard, J., Lemonnier, F., Merad, M., Adema, G., Adams, M., Ferrantini, M., Carpentier, A. F., Escudier, B., Tursz, T., Angevin, E., Zitvogel, L. (2004) Exosomes as potent cell-free peptide-based vaccine. II. Exosomes in CpG adjuvants efficiently prime naive Tc1 lymphocytes leading to tumor rejection. *J. Immunol.* **172,** 2137–2146.
7. Thery, C., Duban, L., Segura, E., Veron, P., Lantz, O., Amigorena, S. (2002) Indirect activation of naive CD4+ T cells by dendritic cell-derived exosomes. *Nat. Immunol.* **3,** 1156–1162.
8. Andre, F., Chaput, N., Schartz, N. E., Flament, C., Aubert, N., Bernard, J., Lemonnier, F., Raposo, G., Escudier, B., Hsu, D. H., Tursz, T., Amigorena, S., Angevin, E., Zitvogel, L. (2004) Exosomes as potent cell-free peptide-based vaccine. I. Dendritic cell-derived exosomes transfer functional MHC class I/peptide complexes to dendritic cells. *J. Immunol.* **172,** 2126–2136.
9. Segura, E., Amigorena, S., Thery, C. (2005) Mature dendritic cells secrete exosomes with strong ability to induce antigen-specific effector immune responses. *Blood Cells Mol. Dis.* **35,** 89–93.
10. Segura, E., Nicco, C., Lombard, B., Veron, P., Raposo, G., Batteux, F., Amigorena, S., Thery, C. (2005) ICAM-1 on exosomes from mature dendritic cells is critical for efficient naive T-cell priming. *Blood* **106,** 216–223.
11. Viaud, S., Ploix, S., Lapierre, V., Thery, C., Commere, P. H., Tramalloni, D., Gorrichon, K., Virault-Rocroy, P., Tursz, T., Lantz, O., Zitvogel, L., Chaput, N. (2011) Updated technology to produce highly immunogenic dendritic cell-derived exosomes of clinical grade: a critical role of interferon-γ. *J. Immunother.* **34,** 65–75.
12. Thery, C., Regnault, A., Garin, J., Wolfers, J., Zitvogel, L., Ricciardi-Castagnoli, P., Raposo, G., Amigorena, S. (1999) Molecular characterization

←

Figure 4. Heterogeneity in MHCII contents of EVs secreted in cultures of DC only and cognate DC–T cell cocultures. CFSE-labeled T cells were cultured alone or in coculture with nonlabeled, LPS-stimulated, peptide-pulsed DCs for 24 h. T cells were gated based on CFSE staining and analyzed for MHCII, TCR, or CD69 by flow cytometry. The levels of the indicated proteins detected on T cells in cognate cocultures were calculated relative to those found on T cells cultured alone (set to 1). Indicated are the average values ± SD of three individual experiments. (B–D) DC-derived EVs were labeled and analyzed as described in Fig. 3. (B) Dot plots representing PKH67 and anti-MHCII antibody-labeled EVs derived from cultures of LPS-stimulated DCs (left) or cognate DC/LPS–T cell cocultures (right). Based on isotype control stainings, quadrants were set in such a way that upper-right quadrants contained only MHCII-positive DC EVs. Arbitrary gates indicate MHCII-lo (lower 20% of positive population), -int, and -high (upper 10% of positive population) MHCII levels on DC/LPS-derived EVs. The increase in MHCII-negative events in the right plot represents T cell-derived EVs. (C and D) Time-based quantification of MHCII-hi, MHCII-int, or MHCII-lo events detected in different gradient fractions of LPS-stimulated DCs cultured alone (gray diamonds) or in the presence of cognate T cells (black triangles). Indicated are the numbers of events in different gradient fractions measured in 30 s. The data shown in C are from one representative experiment. The data shown in D represent ratios of the number of EVs with different levels of MHCII in culture supernatants of cognate DC/LPS–T cell cultures over those in cultures of LPS-stimulated DCs alone. Indicated are average values ± SD of seven independent experiments. $*P < 0.05$; $**P < 0.01$; $***P < 0.001$.

of dendritic cell-derived exosomes. Selective accumulation of the heat shock protein hsc73. *J. Cell Biol.* **147,** 599–610.
13. Muntasell, A., Berger, A. C., Roche, P. A. (2007) T cell-induced secretion of MHC class II-peptide complexes on B cell exosomes. *EMBO J.* **26,** 4263–4272.
14. Qazi, K. R., Gehrmann, U., Domange Jordo, E., Karlsson, M. C., Gabrielsson, S. (2009) Antigen-loaded exosomes alone induce Th1-type memory through a B-cell-dependent mechanism. *Blood* **113,** 2673–2683.
15. Arita, S., Baba, E., Shibata, Y., Niiro, H., Shimoda, S., Isobe, T., Kusaba, H., Nakano, S., Harada, M. (2008) B cell activation regulates exosomal HLA production. *Eur. J. Immunol.* **38,** 1423–1434.
16. Buschow, S. I., Nolte-'t Hoen, E. N., van Niel, G., Pols, M. S., ten Broeke, T., Lauwen, M., Ossendorp, F., Melief, C. J., Raposo, G., Wubbolts, R., Wauben, M. H., Stoorvogel, W. (2009) MHC II in dendritic cells is targeted to lysosomes or T cell-induced exosomes via distinct multivesicular body pathways. *Traffic* **10,** 1528–1542.
17. Nolte-'t Hoen, E. N., van der Vlist, E. J., Aalberts, M., Mertens, H. C., Bosch, B. J., Bartelink, W., Mastrobattista, E., van Gaal, E. V., Stoorvogel, W., Arkesteijn, G. J., Wauben, M. H. (2012) Quantitative and qualitative flow cytometric analysis of nanosized cell-derived membrane vesicles. *Nanomedicine* **8,** 712–720.
18. Van der Vlist, E. J., Nolte-'t Hoen, E. N., Stoorvogel, W., Arkesteijn, G. J., Wauben, M. H. (2012) Fluorescent labeling of nano-sized vesicles released by cells and subsequent quantitative and qualitative analysis by high-resolution flow cytometry. *Nat. Protoc.* **7,** 1311–1326.
19. Lutz, M. B., Kukutsch, N., Ogilvie, A. L., Rossner, S., Koch, F., Romani, N., Schuler, G. (1999) An advanced culture method for generating large quantities of highly pure dendritic cells from mouse bone marrow. *J. Immunol. Methods* **223,** 77–92.
20. Lauwen, M. M., Zwaveling, S., de Quartel, L., Ferreira Mota, S. C., Grashorn, J. A., Melief, C. J., van der Burg, S. H., Offringa, R. (2008) Self-tolerance does not restrict the CD4+ T-helper response against the p53 tumor antigen. *Cancer Res.* **68,** 893–900.
21. Raposo, G., Nijman, H. W., Stoorvogel, W., Liejendekker, R., Harding, C. V., Melief, C. J., Geuze, H. J. (1996) B lymphocytes secrete antigen-presenting vesicles. *J. Exp. Med.* **183,** 1161–1172.
22. Barois, N., Forquet, F., Davoust, J. (1997) Selective modulation of the major histocompatibility complex class II antigen presentation pathway following B cell receptor ligation and protein kinase C activation. *J. Biol. Chem.* **272,** 3641–3647.
23. Kessler, R. J., Fanestil, D. D. (1986) Interference by lipids in the determination of protein using bicinchoninic acid. *Anal. Biochem.* **159,** 138–142.
24. Soo, C. Y., Song, Y., Zheng, Y., Campbell, E. C., Riches, A. C., Gunn-Moore, F., Powis, S. J. (2012) Nanoparticle tracking analysis monitors microvesicle and exosome secretion from immune cells. *Immunology* **136,** 192–197.
25. Nolte-'t Hoen, E. N., Buschow, S. I., Anderton, S. M., Stoorvogel, W., Wauben, M. H. (2009) Activated T cells recruit exosomes secreted by dendritic cells via LFA-1. *Blood* **113,** 1977–1981.
26. Segura, E., Guerin, C., Hogg, N., Amigorena, S., Thery, C. (2007) CD8+ dendritic cells use LFA-1 to capture MHC-peptide complexes from exosomes in vivo. *J. Immunol.* **179,** 1489–1496.

KEY WORDS:
exosomes · microvesicles · immune regulation · single vesicle analysis · cognate interaction · MHC class II